



# Pancreatic MRI associated with pancreatic fibrosis and postoperative fistula: comparison between pancreatic cancer and non-pancreatic cancer tissue



Y. Noda<sup>a,\*</sup>, S. Goshima<sup>a</sup>, N. Suzui<sup>b</sup>, T. Miyazaki<sup>b</sup>, K. Kajita<sup>a</sup>, H. Kawada<sup>a</sup>,  
N. Kawai<sup>a</sup>, Y. Tanahashi<sup>a</sup>, M. Matsuo<sup>a</sup>

<sup>a</sup> Department of Radiology, Gifu University, 1-1 Yanagido, Gifu, 501-1194, Japan

<sup>b</sup> Department of Pathology, Gifu University Hospital, 1-1 Yanagido, Gifu, 500-1194, Japan

## ARTICLE INFORMATION

### Article history:

Received 24 October 2017

Accepted 20 February 2019

**AIM:** To evaluate the potential value of magnetic resonance imaging (MRI) for predicting postoperative pancreatic fistula (POPF) in patients with pancreatic cancer (PC) and non-pancreatic cancer (non-PC).

**MATERIAL AND METHODS:** This retrospective study was approved by the institutional review board and written informed consent was waived. Forty patients underwent pancreatoduodenectomy due to PC ( $n=31$ ) and non-PC ( $n=9$ ). The pancreas-to-muscle signal intensity ratio (SIR) on three-dimensional (3D)-fast field echo (FFE) T1-, in- and opposed-phase T1-, and T2-weighted images, as well as the apparent diffusion coefficient (ADC) value of the pancreas were measured. The frequency of POPF and MRI measurements were compared between patients with PC and non-PC. The MRI measurements were also compared with the grade of pancreatic fibrosis on pathological findings, fat deposition, and interstitial oedema.

**RESULTS:** The frequency of POPF was significantly higher in patients with non-PC than in those with PC ( $p=0.0067$ ), with an odds ratio of 10.4. The SIR on 3D-FFE T1-weighted images was significantly higher in patients with non-PC ( $p=0.0001$ ) and those with POPF ( $p=0.017$ ) than in those with PC and those without POPF, respectively. Multiple regression analysis demonstrated that the SIR on 3D-FFE T1-weighted image was independently associated with the grade of pancreatic fibrosis ( $p<0.0001$ ).

**CONCLUSION:** The frequency of POPF was significantly higher in patients with non-PC than in those with PC was inversely related to the grade of pancreatic fibrosis. The SIR on 3D-FFE T1-weighted image might be a potential imaging biomarker for predicting POPF.

© 2019 The Royal College of Radiologists. Published by Elsevier Ltd. All rights reserved.

## Introduction

Postoperative pancreatic fistula (POPF) is the most critical complication after pancreatoduodenectomy because it

\* Guarantor and correspondent: Y. Noda. Tel.: +58 230 6437; fax: +58 230 6440.

E-mail address: [noda1031@gifu-u.ac.jp](mailto:noda1031@gifu-u.ac.jp) (Y. Noda).

potentially causes vascular injury, followed by rupture of a pseudoaneurysm.<sup>1,2</sup> Several risk factors were reported to be associated with the frequency of POPF; these include male sex, old age, increased body mass index, narrow diameter of the main pancreatic duct, soft pancreatic parenchyma, presence of fatty pancreas, long duration of the surgical procedure, and high volume of intraoperative blood loss.<sup>3</sup> A previous study demonstrated that the frequency of POPF was lower in cases that had a soft pancreas with ampullary cancer or those with bile duct cancer, compared with cases that had a relatively hard pancreas with pancreatic cancer (PC).<sup>4</sup>

PC is well known to cause pancreatic fibrosis more frequently than distal bile duct, ampullary, and duodenal cancers.<sup>5</sup> In patients with PC, two major mechanisms of paraneoplastic pancreatic fibrosis were reported.<sup>6,7</sup> First, the PC cells activate the surrounding pancreatic stellate cells (PSCs); this activation leads to fibrosis of the tumour and pancreatic tissues.<sup>6,7</sup> Second, the PC cells that originate from the pancreatic ductal epithelial cells can easily obstruct the tiny ductules; consequently, obstructive pancreatitis can be frequent and cause a desmoplastic reaction in the pancreatic tissue.<sup>6,7</sup>

Previous studies demonstrated that the signal intensity of the pancreas on T1-weighted images decreased constantly as pancreatic fibrosis progressed.<sup>8,9</sup> It was postulated that MRI signals would reflect changes in the paraneoplastic pancreatic tissue and may differ between patients with PC and those with non-PC or between those with POPF and those without POPF. Hence, the purpose of the present study was to evaluate the potential value of MRI in predicting POPF in patients with PC and non-PC.

## Materials and methods

### Patients

This retrospective study was approved by the institutional review board and written informed consent was waived. From October 2010 to March 2017, 42 consecutive patients underwent MRI before pancreatoduodenectomy to evaluate local tumour extension and tumour staging. Two patients were excluded because the necessary sequences for the evaluation were not obtained. Therefore, the remaining 40 patients (mean age, 69.9±7.9 [means±1 standard deviation] years; age range, 52–82 years), including 23 men (mean age, 69.4±9.0 years; range, 52–82 years) and 17 women (mean age, 70.6±6.4 years; range, 58–81 years), comprised the study cohort (Fig 1).

MRI of the pancreas was performed using a 1.5-T (Intera Achieva Nova Dual; Philips Medical Systems, Best, the Netherlands) and 3-T MRI system (Intera Achieva Quasar Dual; Philips Medical Systems, Best, the Netherlands) using a six-channel torso array coil. The basic MRI protocol and imaging parameters are summarised in Table 1.

### Reference standard

The interval between preoperative MRI and pancreatoduodenectomy ranged from 1 to 91 days (mean, 34

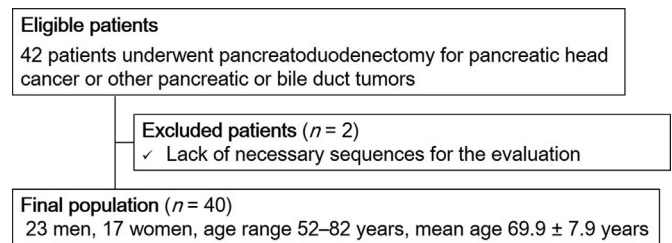


**Figure 1** Flow diagram of study enrollment population. Mean age is means±1 standard deviation.

days). In the 40 patients, the histopathological diagnoses were pancreatic head adenocarcinoma ( $n=31$ ), intra-ductal papillary mucinous carcinoma ( $n=2$ ), extrahepatic bile duct carcinoma ( $n=2$ ), ampullary carcinoma ( $n=2$ ), intraductal papillary mucinous neoplasm ( $n=1$ ), mucinous cystic adenoma ( $n=1$ ), and paraganglioma ( $n=1$ ).

For the assessment of pancreatic fibrosis, the non-tumoural pancreatic tissues abutting the resected area were evaluated by an experienced pathologist (N.S. with 19 years of experience in oncologic pathology). Azan staining was performed to grade the proliferation of the collagenous materials contributing to pancreatic fibrosis; specimens stained with haematoxylin–eosin were used to grade the degrees of fat deposition and interstitial oedema in the non-tumoural pancreatic parenchyma distal to the lesion. The grading criteria for pancreatic fibrosis were as follows<sup>10</sup>: F0=normal pancreatic parenchyma, no fibrotic changes; F1=mild fibrous tissue; F2=moderate fibrosis with marked sclerosis of interlobular septa and no evidence of architectural changes; and F3=severe fibrosis with architectural destruction. The grading criteria for fat deposition were as follows<sup>9</sup>: L0=0–10% deposition in the pancreatic parenchyma ( $\times 40$  magnification); L1=11–20%; L2=21–30%; and L3=>31%. The grading criteria for interstitial oedema were as follows<sup>8</sup>: E0=no or slight interstitial oedema ( $\times 40$  magnification); E1=mild periductal or interlobular oedema; E2=moderate periductal or interlobular oedema; and E3=severe periductal or interlobular oedema.

The development of POPF was defined according to the definition of the International Study Group for Pancreatic Society.<sup>11</sup> POPF was diagnosed as amylase content in the drainage fluid on or after postoperative day 3 of greater than three times the upper limit of the normal serum value. All patients were followed up based on the amylase level in the drainage fluid and the serum amylase levels on postoperative days 1, 3, and 5. Three different grades of POPF (grades A, B, and C) were defined according to the clinical impact on the patient's hospital course: grade A required few changes in treatment or deviation from the normal clinical pathway; grade B required some changes in treatment or adjustment in the clinical pathway, such as prolonged drainage or specific medical treatment; and grade C required invasive treatment.

**Table 1**  
MRI sequences and parameters.

Parameter	1.5-T				3-T			
	T1WI	In/out	T2WI	DWI	T1WI	In/out	T2WI	DWI
Sequence	3D FFE	GRE	2D TSE	2D EP	3D FFE	GRE	2D TSE	2D EP
Respiratory control	BH	BH	RT	FB	BH	BH	RT	BH
Fat suppression	Yes	No	Yes	Yes	Yes	No	Yes	Yes
TR (ms)	160	223	1,200	1,371	160	242	1,600	2,292
TE (ms)	4.1	4.6/2.3	80	49	4.1	2.3, 4.6/1.1, 3.5	80	46
Flip angle (degree)	75	80	90	90	75	60	90	90
FOV (cm)	38×30	38×30	38×30	38×30	38×30	38×30	38×30	38×30
Matrix	320×224	320×224	320×224	128×90	320×224	288×230	512×256	112×90
Parallel imaging factor	1.1	1.6	1.6	2.0	1.1	2.2	2.0	3.0
Section thickness (mm)	5	5	5	7	5	5	5	6
Intersection gap (mm)	1	1	1	0	1	1	1	0
No. of sections	30	30	30	30	30	30	30	30
Acquisition time	24 s	23.4 s	4 min	1 min 7 s	24 s	21 s	3 min	41.2 s
b-values (mm <sup>2</sup> /s)	NA	NA	NA	0, 500	NA	NA	NA	0, 500

T1WI, T1-weighted imaging; T2WI, T2-weighted imaging; DWI, diffusion-weighted imaging; 3D, three dimensional; 2D, two dimensional; FFE, fast field-echo; GRE, gradient recalled-echo; TSE, turbo spin-echo; EP, echo-planar; BH, breath-hold; RT, respiratory-triggered; FB, free-breathing; TR, repetition time; TE, echo time; FOV, field of view; NA, not applicable.

### Quantitative image analysis

The operation time and intraoperative blood loss were recorded from the hospital information. Two radiologists (Y.N. and N.K., with 7 and 6 years, respectively, of post-training experience of interpreting abdominal MRI images) who had no knowledge of the patients' clinical or histopathological information measured in consensus the signal intensities of the pancreatic parenchyma ( $SI_{\text{pancreas}}$ ) and paraspinal muscle ( $SI_{\text{muscle}}$ ) on three-dimensional (3D)-fast field echo (FFE) T1-, in- and opposed-phase T1-, and T2-weighted images in order to calculate the signal intensity ratio ( $SIR=SI_{\text{pancreas}}/SI_{\text{muscle}}$ ). The apparent diffusion coefficient (ADC) values of the pancreatic parenchyma were also calculated.

For each measurement, a circular region of interest (ROI; 50–150 mm<sup>2</sup>) was placed at the side of the pancreatic head adjacent to the resection plane in order to match, as closely as possible, the locations of the surgical specimen on histopathological evaluation, with reference to postoperative images; the ROI was devoid of dilated pancreatic duct, vessels, or artefacts. The radiologists were allowed to zoom in the images during ROI measurements of atrophic pancreatic tissues. For all measurements, the size, shape, and position of the ROI were kept constant among all MRI images by applying a copy-and-paste function on the viewer. If the ROI was placed in an inadequate location among the different sequences, the radiologists carefully adjusted the location of the ROIs.

### Statistical analysis

Statistical analyses were performed using MedCalc Software for Windows (version 16.8.4). The Mann–Whitney *U* and Fisher's exact tests were conducted to evaluate differences in patients' age, gender, body mass index (BMI), operation time, intraoperative blood loss, and the proportion of PC and non-PC between patients with and those

without POPF. The Mann–Whitney *U* test was conducted to evaluate differences in grade of pancreatic fibrosis, fat deposition, and interstitial oedema, as well as differences in the MRI measurements between patients with PC and those with non-PC.

Spearman's rank correlation tests were conducted to evaluate the relationship between the MRI measurements and the grades of pancreatic fibrosis, fat deposition, and interstitial oedema. Ordinal logistic regression analyses were conducted to evaluate the relationship of the MRI measurements with the grades of pancreatic fibrosis, fat deposition, and interstitial oedema. Kruskal–Wallis test with post-hoc tests as described by Conover<sup>12</sup> was conducted subsequently to compare the grade of the pathological changes with the statistically associated MRI measurements. The area under the receiver operating characteristic (ROC) curve (AUC) was calculated for differentiating patients with POPF and those without POPF. The optimal threshold that yielded the highest Youden index was determined, and the sensitivity and specificity were then calculated. A post-hoc power analysis was conducted to assess the ability to detect differences between patients with PC and those with non-PC using commercially available software (G\*Power, version 3.1.7; University of Dusseldorf, Dusseldorf, Germany) with an effect size of 0.30, which is a medium effect, a significance level of 5%, and a total sample size of 40 patients. A *p*-value of <0.05 was defined as significant.

### Results

The patients' background factors are summarised in Table 2. Eleven patients (27.5%) in the study population developed grade A POPF. No significant differences were observed between patients with POPF and those without POPF in terms of age, gender, BMI, operation time, and intraoperative blood loss. The proportion of non-PC

cases was significantly higher in patients with POPF (54.5%) than in those without POPF (10.3%;  $p=0.0067$ ). The patients with non-PC demonstrated an odds ratio of 10.4 (95% confidence interval: 1.9–56) for developing POPF.

The histopathologic grade, SIR, ADC value, and frequency of POPF between patients with PC and those with non-PC are summarised in Table 3. For histopathologic grade, fibrosis grade ( $p=0.019$ ) and fat deposition ( $p=0.012$ ) were significantly lower in patients with non-PC than in those with PC. The SIR on 3D-FFE T1-weighted images ( $p=0.0001$ ), in-phase ( $p=0.011$ ) and opposed-phase ( $p=0.043$ ) T1-weighted images, and ADC value ( $p=0.0042$ ) were significantly higher in patients with non-PC than in those with PC (Fig 2).

The relationships between the MRI measurements and the grades of pancreatic fibrosis, fat deposition, and interstitial oedema are summarised in Table 4. The Spearman rank correlation test showed that the SIR on 3D-FFE T1-weighted images ( $r=-0.63$ ,  $p<0.0001$ ); in-phase ( $r=-0.44$ ,  $p=0.0042$ ) and opposed-phase T1-weighted images ( $r=-0.36$ ,  $p=0.023$ ); and ADC value ( $r=-0.49$ ,  $p=0.0012$ ) were significantly correlated with the grade of pancreatic fibrosis. The ADC value was correlated with the interstitial oedema grade ( $r=-0.33$ ,  $p=0.041$ ). No significant correlation was found between other MRI measurements and the histopathologic grades of fat deposition ( $p=0.13$ ) and interstitial oedema

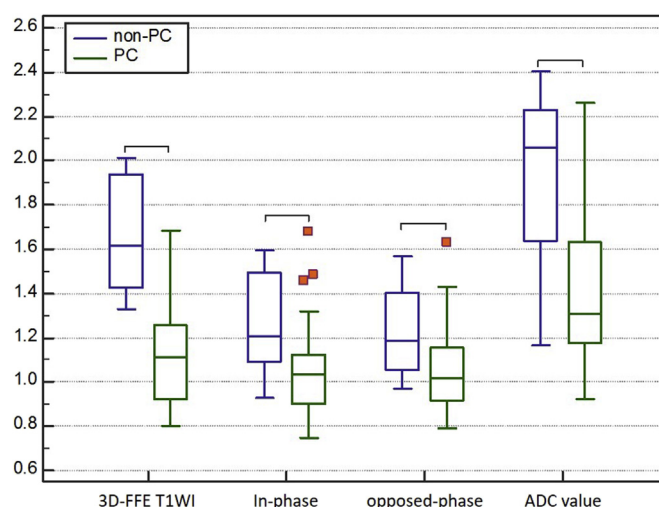


**Figure 2** Boxplot showing the SIRs on 3D T1-weighted FFE images, in- and opposed-phase T1-weighted images, and ADC value in patients with PC and non-PC. The SIR on 3D T1-weighted FFE images, in- and opposed-phase T1-weighted images, and ADC value in patients with non-PC were significantly higher than those with PC. Note that the boundaries of boxes closest to zero are the 25th percentile, lines in boxes are the medians, boundaries of boxes farthest to zero are the 75th percentile, error bars are the smallest and largest values in 1.5 box lengths of 25th and 75th percentiles, and dots are defined as a value that is larger than the upper quartile plus three times the interquartile range.

**Table 2**  
Patients background factors.

	POPF positive	POPF negative	p-Value
Case number	11	29	NA
Patients age	70.8±6.5 (58.0–80.0)	69.6±8.5 (52.0–82.0)	0.95
Male: female	8:3	15:14	0.30
BMI	21.3±10.9 (17.1–27.7)	21.1±3.1 (15.2–27.4)	0.69
Operation time (min)	396.9±53.7 (292.0–486.0)	479.6±108.0 (350.0–750.0)	0.054
Intraoperative blood loss (mL)	823.2±334.0 (250.0–1415.0)	1091.0±816.4 (145.0–3210.0)	0.68
PC: non-PC	5:6	26:3	0.0067*

Data are means ± 1 standard deviation with ranges in parentheses; NA, not applicable; POPF, postoperative pancreatic fistula; BMI, body mass index. \* $p<0.05$ , significant difference.

**Table 3**  
Comparison of grades for pancreatic fibrosis, fat deposition, and interstitial oedema, and magnetic resonance imaging measurements between pancreatic cancer and non-pancreatic cancer cases.

Parameter	Pancreatic cancer	Non-pancreatic cancer	p-Value
<b>Histopathological grades</b>			
Fibrosis	2.32±0.87 (0.00–3.00)	1.44±1.01 (0.00–3.00)	0.019*
Fat deposition	1.06±0.93 (0.00–3.00)	0.33±1.00 (0.00–3.00)	0.012*
Interstitial oedema	1.42±1.09 (0.00–3.00)	1.89±0.93 (0.00–3.00)	0.26
<b>Signal intensity ratio</b>			
3D-FFE T1-weighted imaging	1.12±0.24 (0.80–1.68)	1.66±0.27 (1.33–2.01)	0.0001*
In-phase T1-weighted imaging	1.06±0.21 (0.75–1.68)	1.28±0.24 (0.93–1.59)	0.011*
Opposed-phase T1-weighted imaging	1.07±0.20 (0.79–1.63)	1.21±0.21 (0.97–1.57)	0.043*
T2-weighted imaging	2.85±0.88 (1.43–5.17)	2.33±0.66 (1.64–3.49)	0.10
ADC value	1.40±0.29 (0.92–2.26)	1.91±0.45 (1.17–2.40)	0.0042*

Data are means±1 standard deviation with ranges in parentheses.

\* $p<0.05$ , significant difference.

FFE, fast field-echo. ADC, apparent diffusion coefficient.

**Table 4**  
Correlation of magnetic resonance imaging (MRI) measurements with grades for pancreatic fibrosis, fat deposition, and interstitial edema.

MRI measurements	Pancreatic fibrosis		Fat deposition		Interstitial oedema	
	r value	p-Value	r value	p-Value	r value	p-Value
Signal intensity ratio						
3D-FFE T1-weighted imaging	−0.63	< 0.0001	−0.013	0.94	−0.29	0.076
In-phase T1-weighted imaging	−0.44	0.0042	0.0049	0.98	−0.10	0.53
Opposed-phase T1-weighted imaging	−0.36	0.023	−0.16	0.33	−0.16	0.31
T2-weighted imaging	0.22	0.17	0.20	0.23	0.24	0.13
ADC value	−0.49	0.0012	−0.24	0.14	−0.33	0.041

FFE, fast field-echo. ADC, apparent diffusion coefficient.

( $p=0.98$ ). Ordinal logistic regression analysis showed that the SIR on 3D-FFE T1-weighted images was independently associated with the grade of pancreatic fibrosis (coefficient=−2.06,  $p<0.0001$ ). The other parameters were not significant. The mean SIR on 3D-FFE T1-weighted images gradually decreased as the grade of pancreatic fibrosis progressed ( $p<0.0001$ ). The mean SIR on 3D-FFE T1-weighted images was significantly lower in cases of grade F3 pancreatic fibrosis than in those with grades F0, 1, and 2 ( $p<0.05$ ) and was also significantly lower in F2 cases than in F1 cases ( $p<0.05$ ; Figs 3–5). No significant difference was found in the SIR on 3D-FFE T1-weighted images between cases with grade F0 and those with grade F1 pancreatic fibrosis.

For predicting the development of POPF, the SIR on 3D-FFE T1-weighted images, with a cut-off value of 1.11, yielded a sensitivity of 91%, specificity of 55%, and AUC of 0.75. Post-hoc power analysis demonstrated that there was 19% power to detect an effect size of 0.3 between patients with PC and those with non-PC.

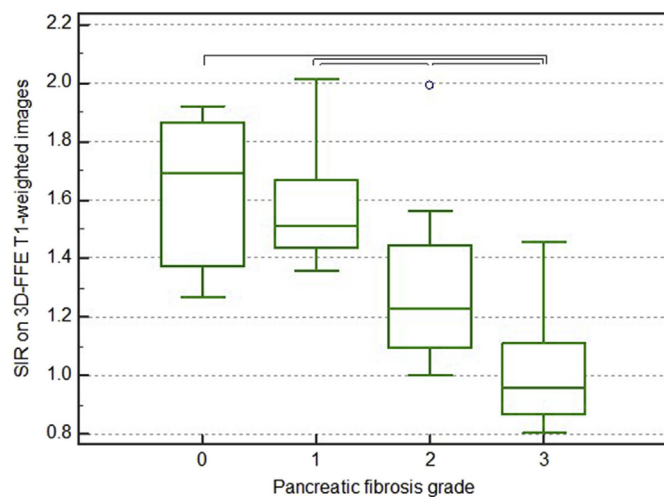


**Figure 3** Boxplot showing the signal intensity ratio on 3D T1-weighted FFE images for pancreatic fibrosis grade. Horizontal brackets indicate the significant differences ( $p<0.05$ ). Note that the boundaries of boxes closest to zero are the 25th percentile, lines in boxes are the medians, boundaries of boxes farthest to zero are the 75th percentile, error bars are the smallest and largest values in 1.5 box lengths of 25th and 75th percentiles, and dots are defined as a value that is larger than the upper quartile plus three times the interquartile range.

## Discussion

Soft pancreatic parenchymal tissue has been reported previously as one of the significant risk factors for developing POPF, which has an incidence of approximately 5% in chronic pancreatitis, 12% in PC, 15% in ampullary cancer, and 33% in bile duct cancer.<sup>13</sup> The present results supported the previous findings that the frequency of POPF was significantly higher in patients with non-PC than in those with PC. The grade of pancreatic fibrosis was significantly lower in patients with non-PC than in those with PC. It was assumed that the present results were based on the strong association between pancreatic fibrosis and PC, which has already been reported as a result of activation of PSCs and secondary to pancreatic ductal obstruction or pancreatitis.<sup>13</sup>

Stepwise multiple regression analysis demonstrated that the SIR on 3D-FFE T1-weighted images was independently associated with the grade of pancreatic fibrosis and that there was no significant correlation between any of the MRI measurements and the grades of fat deposition or interstitial oedema, except for the marginal correlation between the ADC value and grade of interstitial oedema. It is well

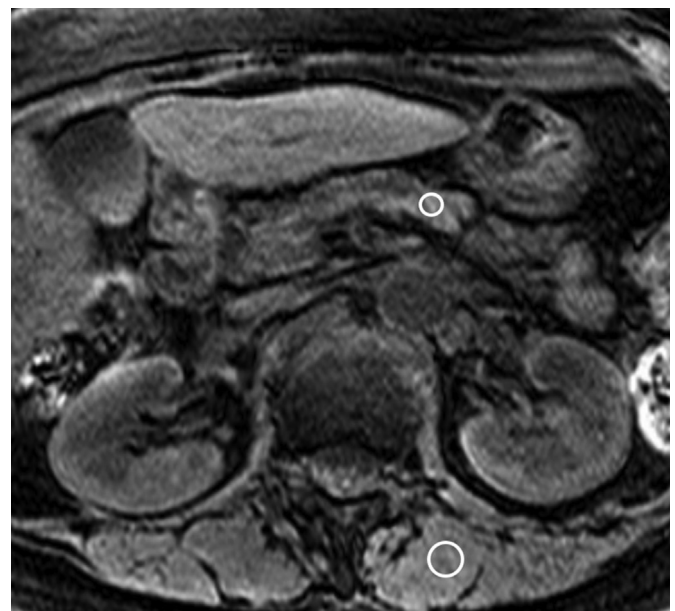


**Figure 4** Axial 3D T1-weighted FFE image in a 73-year-old woman with pancreatic head cancer. Histopathological examination showed the pancreatic fibrosis grade of F3. The signal intensity ratio was 0.92.

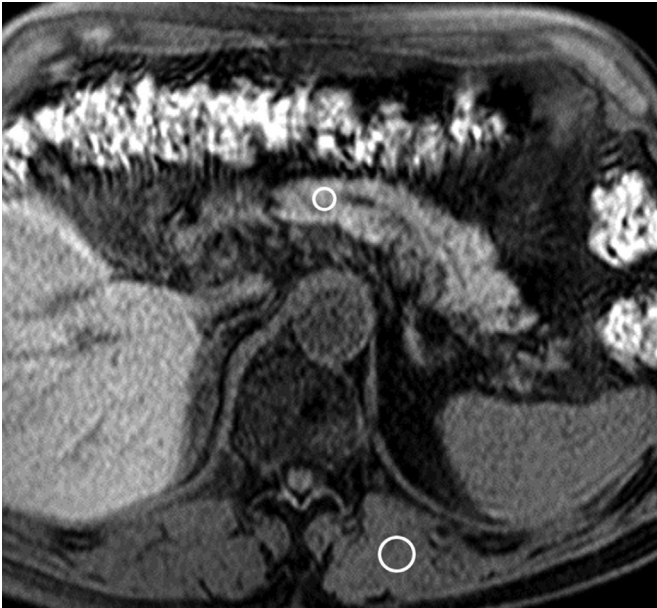


**Figure 5** Axial 3D T1-weighted FFE image in a 74-year-old man with ampullary cancer. Histopathological examination showed the pancreatic fibrosis grade of F1. The signal intensity ratio was 1.62.

known that normal pancreatic parenchyma exhibits relative hyperintensity on T1-weighted images because the pancreatic juice is rich in glycoproteins and the endoplasmic reticulum within the pancreatic cells contribute to the T1 shortening effect<sup>14,15</sup>; however, the signal intensity of the pancreas on T1-weighted images gradually decreases with progression of pancreatic atrophy, fibrosis, interstitial oedema, or fat deposition.<sup>8</sup> According to the present results of multiple regression analysis, the decreased SIR on 3D-FFE T1-weighted images was mainly caused by pancreatic fibrosis, rather than by fat deposition or interstitial oedema.

A previous report also demonstrated that the pancreatic ADC value was significantly lower in patients with acute pancreatitis than in controls.<sup>16</sup> Another report discussed that there might be several reasons for the decreased ADC value observed in acute pancreatitis; these include acinar cell death, invasion of the acinar space by polymorphonuclear leukocytes, deposition of fibrin in intercellular spaces, and microthrombi in blood vessels.<sup>17</sup> In the present study, there was a negative weak correlation between the ADC value and the grade of interstitial oedema grade on univariate analysis. ADC may be a possible biomarker for estimating the degree of pancreatitis or interstitial oedema.

According to the present results, the SIR on 3D-FFE T1-weighted images and the ADC value reflected pancreatic fibrosis and interstitial oedema, respectively. These results support the development of paraneoplastic pancreatic fibrosis in patients with PC. Therefore, pancreatic fibrosis is more frequently caused by PSC activation and/or obstructive pancreatitis in patients with PC than in those with non-PC. In any case, pancreatic fibrosis was strongly associated with POPF and the SIR on 3D-FFE T1-weighted images, rather than the ADC value, was more strongly correlated with POPF.

The present study had several limitations. First, the single-centre, retrospective study design with a relatively small sample size might have caused selection bias. Further prospective clinical studies need to be performed on a larger population to validate the present results. Second, free-breathing diffusion-weighted images were used. The respiratory motion-related artefacts may have incurred a certain degree of errors in the measurements of the ADC value.

In conclusion, the frequency of POPF was significantly higher in patients with non-PC than in those with PC and was inversely related to the grade of pancreatic fibrosis. The SIR on the 3D-FFE T1-weighted images might be a potential imaging biomarker for predicting POPF.

## Conflicts of interest

The authors declare no conflict of interest.

## References

- Fuks D, Piessen G, Huet E, et al. Life-threatening postoperative pancreatic fistula (grade C) after pancreaticoduodenectomy: incidence, prognosis, and risk factors. *Am J Surg* 2009;**197**(6):702–9.
- Tani M, Kawai M, Yamaue H. Intraabdominal hemorrhage after a pancreatectomy. *J Hepatobiliary Pancreat Surg* 2008;**15**(3):257–61.
- Kiyochi H, Matsukage S, Nakamura T, et al. Pathologic assessment of pancreatic fibrosis for objective prediction of pancreatic fistula and management of prophylactic drain removal after pancreaticoduodenectomy. *World J Surg* 2015;**39**(12):2967–74.
- Yang YM, Tian XD, Zhuang Y, et al. Risk factors of pancreatic leakage after pancreaticoduodenectomy. *World J Gastroenterol* 2005;**11**(16):2456–61.
- Erkan M, Hausmann S, Michalski CW, et al. How fibrosis influences imaging and surgical decisions in pancreatic cancer. *Front Physiol* 2012;**3**:389.
- Tanaka T, Ichiba Y, Fujii Y, et al. New canine model of chronic pancreatitis due to chronic ischemia with incomplete pancreatic duct obstruction. *Digestion* 1988;**41**(3):149–55.
- Kloppel G, Detlefsen S, Feyerabend B. Fibrosis of the pancreas: the initial tissue damage and the resulting pattern. *Virchows Arch* 2004;**445**(1):1–8.
- Watanabe H, Kanematsu M, Tanaka K, et al. Fibrosis and postoperative fistula of the pancreas: correlation with MRI findings—preliminary results. *Radiology* 2014;**270**(3):791–9.
- Noda Y, Goshima S, Tanaka K, et al. Findings in pancreatic MRI associated with pancreatic fibrosis and HbA1c values. *J Magn Reson Imag* 2016;**43**(3):680–7.
- Wellner UF, Kayser G, Lapshyn H, et al. A simple scoring system based on clinical factors related to pancreatic texture predicts postoperative pancreatic fistula preoperatively. *HPB (Oxford)* 2010;**12**(10):696–702.
- Bassi C, Dervenis C, Butturini G, et al. Postoperative pancreatic fistula: an international study group (ISGPF) definition. *Surgery* 2005;**138**(1):8–13.
- Conover W. *Practical nonparametric statistics*. 3rd edn. New York, NY: Wiley; 1999.
- Bartoli FG, Arnone GB, Ravera G, et al. Pancreatic fistula and relative mortality in malignant disease after pancreaticoduodenectomy. Review and statistical meta-analysis regarding 15 years of literature. *Anticancer Res* 1991;**11**(5):1831–48.
- Mitchell DG, Vinitzki S, Saponaro S, et al. Liver and pancreas: improved spin-echo T1 contrast by shorter echo time and fat suppression at 1.5 T. *Radiology* 1991;**178**(1):67–71.
- Winston CB, Mitchell DG, Outwater EK, et al. Pancreatic signal intensity on T1-weighted fat saturation MRI images: clinical correlation. *J Magn Reson Imag* 1995;**5**(3):267–71.
- Thomas S, Kayhan A, Lakadamyali H, et al. Diffusion MRI of acute pancreatitis and comparison with normal individuals using ADC values. *Emerg Radiol* 2012;**19**(1):5–9.
- Bockman DE, Buchler M, Beger HG. Ultrastructure of human acute pancreatitis. *Int J Pancreatol* 1986;**1**(2):141–53.